Soil–atmosphere interaction in the overburden of a short-lived low and intermediate level nuclear waste (LLW/ILW) disposal facility

Ni An, Yu-Jun Cui, Nathalie Conil, Jean Talandier, Sebastien Conil

Soil–atmosphere interaction in the overburden of a short-lived low and intermediate level nuclear waste (LLW/ILW) disposal facility

Ni An[1*], Yu-Jun Cui[1], Nathalie Conil[2], Jean Talandier[3], Sebastien Conil[3]

1: Ecole des Ponts ParisTech, Laboratoire Navier/CERMES, 6 et 8 avenue Blaise Pascal, 77455 Marne La Vallée cedex 2, France

2: Andra, Centre de Meuse/Haute-Marne, RD 960, 55290 Bure, France

3: Andra, 1/7, rue Jean Monnet, 92298 Châtenay-Malabry cedex, France

*Corresponding author:

Ni AN

Ecole des Ponts ParisTech, Laboratoire Navier/CERMES, 6 et 8 avenue Blaise Pascal, 77455 Marne La Vallée cedex 2, France

E-mail: ni.an@enpc.fr

Abstract： The long-term safety of shallow disposal facility for short-lived low and intermediate level nuclear waste (LLW/ILW) relies on the performance of engineered barriers (caps and liners). Soil-atmosphere interaction may affect the capping material at shallow depths, due to changes of its coupled hydro-thermal-mechanical behavior under the effect of atmospheric conditions. This study aims to investigate the soil-atmosphere interaction at different time scales in the overburden of an LLW/ILW disposal facility, located in middle France. Actual meteorological data from Valencia El Saler station in Spain, including solar radiation, air temperature, latent heat, rainfall, and actual evaporation, at four different time scales (30 min, daily, weekly and monthly), were applied as the future climate conditions of the studied area based on climate analogues. A numerical approach combining a coupled hydro-thermal model and a soil-atmosphere interaction model was employed. Results show that the employment of meteorological data at a short time scale (30 min) can increase the simulation accuracy by capturing the extreme climate events and accelerating the soil-atmosphere interactions. Furthermore, the effect of future climate conditions in the long-term (7 years) on soil hydro-thermal behavior was examined. This enables a further detailed inspection of the climate's role in the LLW/ILW storage system.

Keywords: Soil-atmosphere interaction; Soil hydro-thermal behavior; Further meteorological information; Different time scales; Long-term estimation

1. Introduction

Nuclear waste is currently being disposed at a number of facilities all over the world [1–3]. Considering the decay of radioactivity, a near-surface type of disposal facility is usually proposed for the short-lived low and intermediate level nuclear waste (LLW and ILW) [4]. By contrast, the solution for the disposal of high-level and other long-lived nuclear waste (HLW) is a deep geological repository [2,5]. In the case of LLW/ILW repository, soil-atmosphere interaction may affect its capping material at shallow depths by the physical process of heat and mass transfer over time. For instance, cracks may be produced as a consequence of long dry and hot periods, significantly modifying the thermo-hydro-mechanical properties of the capping material; contaminant transport in the host geologic formation may be accelerated due to changes in soil temperature, water content and suction from weathering, etc. [6,7]. Hence, the effect of climate change must be considered in the assessment of the long-term performance of LLW/ILW disposal.

Soil–atmosphere interaction drives water, energy and biogeochemical cycles, causing variations of soil moisture, temperature, and suction, etc. [8–10]. Over recent years, increasing awareness about the importance of soil-atmosphere interaction has led researchers to investigate the potential effect of climate change on the performance of waste covers and nuclear waste handing [11–16]. Fischer [13,14] undertook studies to determine the rates and directions of water movement through unsaturated sediments for the assessment of the contaminant movement near an arid LLW disposal facility. Phillips et al. [15] studied the mineral behavior and transformations brought on by climate change may affect the long-term performance of the cap and even the LLW disposal facility. Nasir et al. [16] investigated that both permeability and porosity of the near field sedimentary host rocks for the LLW/ILW disposal increase as a result of climate change. In summary, the evaluation of waste covers in terms of waste isolation and contaminant transport requires details of subsurface

62 flows which are significantly affected by climatic fluctuations. Specifically, the major threat to the
63 integrity of nuclear waste isolation in the near-surface type of disposal facility is the water
64 infiltration due to the potential movement of dissolved and mobilized radioactive constituents.
65 Therefore, considering the long life of radioactive waste, it is of paramount importance to well
66 determine the hydro-geologic characteristics of an LLW/ILW disposal facility in order to limit
67 water flow in the vicinity of the disposal facility [13,14].

68 The soil hydraulic condition in the overburden of LLW/ILW disposal facilities is governed by
69 precipitation and evapotranspiration which are associated with the changing climate conditions.
70 Generally, long-term climatic cycles present a low frequency and small amplitude, having less
71 impact on the capping material. However, the low-frequency extreme weather events, such as a
72 long-term drought, may result in significant damage to cap materials [15,17]. The fundamentals of
73 the safety assessment of waste disposal facilities of LLW/ILW/HLW in Belgium were discussed
74 by van Geet et al. [12], emphasizing the importance of considering climate evolution. However, to
75 the authors' knowledge, no study has been undertaken to investigate the soil-atmosphere
76 interaction in the LLW/ILW overburdens under the effect of future climate conditions.

77 This study aims at better understanding the soil-atmosphere interaction in the overburden of the
78 LLW/ILW disposal facility, through identifying the soil coupled hydro-thermal responses to the
79 future climate changes. A numerical approach combining a coupled hydro-thermal model and a
80 soil-atmosphere interaction model was employed and implemented through the Finite Element
81 Method using FreeFem++ code [18]. Considering climate analogues, actual meteorological data
82 collected from Valencia El Saler station was employed as the future climate condition of the studied
83 site located in middle France. Firstly, the meteorological data in the year 2000 collected at the time
84 intervals of 30 min, daily, weekly, and monthly, were used to investigate the effect of the time scale

of climate conditions on the hydro-thermal behavior of the overburden soil. Moreover, the influence depths in terms of soil water content and temperature at different time scales were examined, respectively. Secondly, the meteorological data at the time scale of 30 min for a longer period from 2000 to 2006 (7 years) was employed to investigate the long-term soil-atmosphere interaction and the influence depths in terms of soil temperature and water content.

2. Investigated site

The studied site which was devoted to the storage of short-lived LLW/ILW was located at Soulaines (Aube), France. Figure 1a plots its stratigraphic profile, including three layers: a layer of nature backfill soil, a 5 m superficial layer and a natural Teguline clay layer of 50 to 70 m thickness. Specifically, the excavated zone is at a depth of -20~-30 m and the storage space for LLW/ILW is at a depth of -25~-35 m.

For further study, the studied region is simplified as three layers with homogeneous soil for each (Figure 1b). The primary soil information of each layer is detailed in Table 1. The soil temperature at the bottom zone of the studied region was measured as 14°C [19]. The local water table was close to the bottom boundary of the natural Teguline clay layer. The soil thermal conductivity, water retention curve and hydraulic conductivity curve of each layer are detailed as follows.

2.1 Layer 1 (L1)

In terms of silt clay as the backfill material of L1, its parameters used for the assumed simulations were estimated from results obtained on a soil comparable to that at the site. The variation of soil thermal conductivity versus its volumetric water content is expressed in a linear relationship by equation (1) [20,21] (Table 2) and plotted in Figure 2a. The soil water retention curve (Figure 2b)

can be described by van Genuchten model [22–24]. The relevant parameters in equation (2) are listed in Table 2. Based on the soil water retention curve, its hydraulic conductivity curve is determined by equation (3) and drawn in Figure 2c. The saturated soil hydraulic conductivity is estimated as 1.0×10^{-8} m/s [25].

2.2 Layer 2 (L2)

KD2 instrument [26] was used herein to measure the thermal conductivity of the compacted Teguline clay. A linear relationship between soil thermal conductivity and volumetric water content is considered to fit the measured results [27,28]. The proposed relationship is expressed by equation (4) and presented in Figure 2a. Similar to the case of L1, van Genuchten model [24] is used to describe the variations of soil water retention and hydraulic conductivity of L2. Based on the measured data obtained by Cuisinier and Masrouri [29], the fitting curve is drawn in Figure 2b, providing the values of van Genuchten model parameters in Table 2. The hydraulic conductivity curve is determined with the measured saturated hydraulic conductivity 1.4×10^{-9} m/s [29] (equation (3) and Figure 2c).

2.3 Layer 3 (L3)

As far as the natural Teguline clay is concerned in L3, the thermal conductivity was measured by Zhang et al. [30], presenting slight variations versus soil dry density and water content. Therefore, its soil thermal conductivity is considered as a constant value of 2 W/(m.K) for the purpose of simplification. Based on the measured data obtained by Zeng et al. [31], the variations of soil water retention and hydraulic conductivity of L3 are described by equations (2) and (3). The fitting curves are plotted in Figures 2b and 2c, respectively. The measured saturated hydraulic conductivity is 3.0×10^{-12} m/s.

129 *2.4 Meteorological information*

130 Hallegatte et al. [32] presented a type of climate relocation based on the concept of spatial climate
131 analogues, which specifies that a location that presently enjoys a climate close to the one another
132 city will experience in the future (the end of the twenty-first century). Based on the acceptable
133 analogues of climate relocation, the studied site in the central part of northern France may
134 experience an eastern Spain type of climate in the future [33,34]. Thereby, the actual
135 meteorological data collected from Valencia El Saler station was employed to represent the future
136 climate conditions that the studied site located in middle France may experience. It is worth noting
137 that in the current knowledge of climate change, the predicted future local climate conditions are
138 always attached with uncertainties due to the limitations of climate models, internal climate system
139 processes and socio-economical, demographic or technological evolutions. The measured solar
140 radiation, air temperature, latent heat, rainfall and the estimated actual evaporation rate from
141 01/01/2000 to 31/12/2000 are plotted in Figure 3 at different time scales (30 min, daily, weekly
142 and monthly respectively). They were used to study the effect of climate conditions at different
143 time scales on the interaction between soil and atmosphere. Figures 3a, 3b, and 3c demonstrate the
144 diurnal and seasonal variations of solar radiation, air temperature, and latent heat, with higher
145 values in the summer period and lower values during the wintertime. However, it is observed that
146 rainfall data does not vary seasonally (Figure 3d). Similar to the results of latent heat, evaporation
147 data presents the highest value in summer (Figure 3e). In addition, the comparison of each climate
148 factor at different time scales suggests that the smaller fluctuations are obtained at a longer time
149 scale. Especially, the extreme climate conditions, such as the highest temperature and the most
150 torrential rainfall events, can be identified at the time scale of 30 min.

151 Furthermore, meteorological information at the time scale of 30 min in the period from
152 01/01/2000 to 31/12/2006 (7 years), was employed to study the long-term soil hydro-thermal
153 behavior (Figure 4) in the future. The annual variations of solar radiation, air temperature, latent
154 heat, rainfall, and the estimated evaporation are plotted in Figures 4a~e, respectively, displaying
155 an apparent seasonality. The peak values of solar radiation (Figure 4a) and air temperature (Figure
156 4b) are observed in summertime and wintertime of each year. Specifically, the magnified image of
157 solar radiation above 800 W/m^2 displays an increasing trend, reflecting the warming climate
158 condition as time continues. The effect of climate change on the variations of latent heat and
159 evaporation is identified by higher values of latent heat and evaporation in the wintertime of years
160 2003, 2004, 2005 and 2006 than those of the years 2000, 2001 and 2002. Besides, more frequent
161 rainfall events (Figure 4d) are recorded in the years 2003, 2004, 2005 and 2006.

162

163 **3. Numerical approach**

164 *3.1 Introduction of the numerical approach*

165 A numerical approach combining a coupled hydro-thermal model and a soil-atmosphere interaction
166 model developed by An et al. [10] was employed in this study. The coupled hydro-thermal model
167 was used to describe the coupled water and heat flow in unsaturated soil. The soil-atmosphere
168 interaction model was applied to describe the continuous water and heat transfer between soil and
169 atmosphere, which can be expressed by energy and mass balance, respectively. Details of the
170 numerical formulation and computational aspects have been presented by An et al. [10], and
171 therefore, they are not repeated herein.

3.2 Model dimensions and boundary conditions

Figure 5 displays the applied model dimensions: BC1 and BC 3 represent the bottom and top boundaries, respectively; BC 2 and BC 4 are the lateral boundaries. The height and width of the studied zone are 71 m and 10 m, respectively.

On the first day of the year 2000, the soil volumetric water content was measured as 5.8% and the soil temperature was 11.67 ℃ at the ground surface. Meantime, the soil temperature was measured to be 14 ℃ at the saturated bottom boundary (BC1). Thereby, the initial conditions about soil temperature and water content/suction were defined in a linear relationship with depth. No water and heat transfer were considered at the lateral boundaries. Based on the soil-atmosphere interaction model, the soil heat flux and evaporation/infiltration were applied as the thermal and hydraulic conditions at the top boundary, respectively. The details are explained as follows:

Energy balance

In the case of heat transfer between soil and atmosphere, solar radiation is usually the only exterior heat resource. Specifically, the net solar radiation equals the sum of latent heat, soil heat, and sensible heat. The energy balance is described by:

$$R_n = G + L_E + H \tag{5}$$

where R_n (W/m^2) is the net solar radiation flux; G (W/m^2) is the soil heat flux; L_E (W/m^2) is the latent heat flux; H (W/m^2) is the sensible heat flux. The net solar radiation at 30 min is estimated by:

$$R_n = (1-\alpha) R_{si} - \left[a_c \left(\frac{R_{si}}{R_{so}} \right) + b_c \right] \left(a_e + b_e e_d^{0.5} \right) \sigma \left(T_a^4 \right) \tag{6}$$

where the solar radiation R_{si} (W/m^2) was measured as shown in Figure 3a; T_a (ºC) is the recorded air temperature (Figure 3b); the definition and values of other parameters were detailed by An et al. [10].

The measured values of latent heat at different time scales are introduced in Figure 3c. Considering the convection of airflow in soil-atmosphere interaction, the sensible heat was estimated following the same method presented by An et al. [10]. With the obtained values of net solar radiation, latent heat and sensible heat fluxes at different time scales, the soil heat flux boundary condition at the soil surface at the corresponding scale can be determined based on equation (5).

Mass balance

In terms of bare soil during rainfalls, water reaches the ground surface and infiltrates into the soil continuously until the rainfall rate exceeds the soil infiltration capacity. In that case, the process of runoff begins. However, it stops as soon as the rate of rainfall becomes lower than the actual rate of infiltration. Meanwhile, evaporation occurs spontaneously due to the gradient in temperature and relative humidity near the soil-atmosphere interface. The mass balance during soil-atmosphere interaction is expressed as:

$$P = I_{nf} + R_{off} + E_a \tag{7}$$

where P (m/s), I_{nf} (m/s), R_{off} (m/s) and E_a (m/s) represent the rainfall, infiltration, runoff and actual evaporation rates on soil surface, respectively. Field rainfall was monitored at different time scales of 30 min, daily, weekly, and monthly (Figure 3d). Around 97% of the measured rainfall rates are less than 5.5 mm/30min, which means that most of the runoff rates are in the range from 0.025 to

210 0.05 mm/30min [35]. Therefore, runoff is considered to be negligible in this study. Actual
211 evaporation rate (Figure 3e) was estimated based on the values of latent heat:

$$E_a = L_E / (\rho_w L_v) \quad (8)$$

212 where L_E (W/m^2) is the latent heat flux (Figure 3c); L_v (J/kg) is the latent heat of water vaporization;
213 ρ_w represents the water density (kg/m^3). With the available information about rainfall and actual
214 evaporation rates, the water flux boundary condition (I_{nf}) at the soil surface can be estimated at
215 different time scales.

216 Firstly, with the meteorological information collected every 30 minutes and soil parameters, the
217 numerical investigation was performed at a time step of 30 min for the year 2000. Afterwards, the
218 simulation scenarios at time scales of daily, weekly and monthly were implemented respectively,
219 at a time step of 1 day, for the year 2000 with the inputting data (rainfall, latent heat, air temperature,
220 and solar radiation, etc.) at the corresponding time scale. Finally, the simulation was carried out at
221 a time step of 30 min for 7 years (from 2000 to 2006) with the meteorological data at the time scale
222 of 30 min.

223

224 **4 Results and discussion**

225 *4.1 Soil hydro-thermal behavior at different time scales in one year (2000)*

226 4.1.1 Soil hydro-thermal behavior at the time scale of 30 min

227 Figures 6a and 6b depict the variations of soil volumetric water content and temperature at depths
228 of 0 m, -0.25 m, -0.5 m, -0.75 m, -1.0 m and -1.5 m in the year 2000. It appears that soil volumetric
229 water content increases significantly in response to rainfall events on 14/01/2000, 20/03/2000,
230 09/06/2000, and 22/10/2000, etc. It keeps a decreasing tendency as the result of evaporation during

231 the drying periods. As the depth increases, soil volumetric water content shows much smaller
232 fluctuations compared to that at near soil surface points (Figures 6a).

233 In terms of the soil temperature at the studied depths, they present a general increasing trend
234 from the winter to the summer, approaching the peak values on 18/08/2000. Afterwards, they start
235 to decline gradually until the end of the year 2000. The distinct seasonal variation of soil
236 temperature is observed with larger values in the summer and lower values in the winter (Figure
237 6b), showing a good agreement with the heat-related climate factors (solar radiation, air
238 temperature, etc.). Similar to the result of soil volumetric water content, the surface soil temperature
239 shows more significant variations compared to other depths.

240 To further explore the influence depth of the soil-atmosphere interaction, the calculated soil
241 volumetric water content and temperature profiles in the zone with depth 0~-21 m are presented in
242 Figures 7a and 7b, respectively. The soil volumetric water content below -4.8 m keeps nearly stable,
243 indicating that the influence depth of climate conditions is limited to this value. Figure 7b shows
244 that the influence depth of climate conditions is limited to 12 m depth in terms of soil temperature.
245 Furthermore, a larger amplitude is identified in the profiles of soil temperature, compared to that
246 of soil volumetric water content, reflecting the significant contribution of the surface thermal
247 boundary conditions. It is therefore necessary to investigate the influence depths of temperature
248 and volumetric water content separately, as suggested by An et al. [10].

249

250 4.1.2 Soil hydro-thermal behavior at different time scales

251 The variations of soil volumetric water content at different time scales (30 min, daily, weekly,
252 and monthly) are plotted for depths 0 m (Figure 8a), -0.25 m (Figure 8b), -0.75 m (Figure 8c), and
253 -1.5 m (Figure 8d), respectively. At each depth, a similar variation tendency is observed among the

254 results of soil volumetric water content at different time scales. Generally, the results at the time
255 scale of 30 min depict the maximum and minimum values, except the unexpected daily results on
256 21/03/2000. In the daily results on the soil surface (Figure 8a), soil water content increases sharply
257 to 35% on 21/03/2000 and then exhibits a general decreasing trend with a few jumps due to rainfall
258 events until 11/06/2000. The daily results show a consistent variation mode as the 30 min results
259 but with a higher value over the dry periods, suggesting the continuous effect of the unexpected
260 daily rainfall data on 21/03/2000. In the same rainfall event, a more significant increase in water
261 content is observed in the 30 min results compared to other results. This suggests that a time scale
262 as short as 30 min is capable of increasing the accuracy of simulation results by accelerating the
263 iteration rate of soil-atmosphere interaction. Furthermore, the daily fluctuations of soil water
264 content are more evident at the time scale of 30 min than others, especially for the period with
265 intense rainfall (23/10/2000 to 31/12/2000).

266 Figure 9 plots the evolutions of the soil temperature at different depths at different time scales
267 (30 min, daily, weekly, and monthly). It appears that at the soil surface, the fluctuations are more
268 significant at the time scale of 30 min than others (Figure 9a). As the studied point goes deeper,
269 the difference between the soil temperatures at different time scales is becoming smaller.

270 The simulated soil volumetric water content and temperature profiles at time scales of daily,
271 weekly and monthly are plotted in Figures 10a, 10b, and 10c, respectively. The influence depths
272 of climate conditions on soil volumetric water content are about 5.2 m, 11.6 m, and 11.6 m at the
273 time scales of daily, weekly, and monthly, respectively. They are larger than that of 30 min (4.8
274 m). This is attributed to the effective mass interaction between soil and atmosphere at the time scale
275 of 30 min. On one hand, rainfall events occur during some specific periods rather than continue at
276 a constant rate for daily/weekly/monthly. Hence, soil water content varies more quickly due to the

277 rainfall at the time scale of 30 min than those of other time scales. On the other hand, due to the
278 monthly average evaporation rate at the soil surface, water content at the time scale of monthly
279 decreases for a longer period compared to others (Figure 8d). Thereby, when the
280 evaporation/rainfall at the time scale of 30 min is applied as the hydraulic boundary condition, they
281 lead to a shallower influenced zone compared to the results of other time scales.

282 On the other hand, similar to that of 30 min results, the influence depths of climate conditions
283 on soil temperature is limited to around 12.0~12.8 m at time scales of daily, weekly, and monthly.
284 The effect of time scale on the influence depth of climate conditions in case of soil temperature is
285 not significant as the results of soil water content. It may be attributed to the participation of soil
286 surface temperature in the estimation of sensible heat and hence the value of heat flux boundary
287 condition, which may lead to the same amount of energy transfer between soil and atmosphere at
288 different time scales. Additional work is required to further clarify this point. In the region below
289 the influenced zone, both soil volumetric water content and temperature remain stable as their real
290 initial conditions during the studied period. It is thereby suggested to measure the real initial soil
291 conditions in the area of interest for the evaluation of LLW/ILW storage system's performance.

292

293 *4.2. Soil long-term hydro-thermal behavior for 7 years (2000-2006)*

294 4.2.1 Variations of soil volumetric water content and temperature

295 Figure 11a plots the changes in soil volumetric water content at different depths (0 m, -0.25 m, -
296 0.75 m, and -1.5 m) from 01/01/2000 to 31/12/2006. It is observed that soil volumetric water
297 content increases because of rainfall and keeps a decreasing tendency due to evaporation in the
298 drying periods. Moreover, soil volumetric water content at the surface point shows much larger
299 fluctuations compared to that of other depths.

The evolutions of the soil temperature at different depths during the studied period are illustrated in Figure 11b. Soil temperatures at these studied points present apparent seasonal variations with larger values during the summer period and smaller values in the wintertime. A larger variation amplitude of soil temperature is also identified at the soil surface than other depths. Moreover, over time, the peak temperature in the summer goes up gradually, evidencing the effect of climate change on soil temperature in the long term.

4.2.2 Influence depths

Soil volumetric water content profiles at different times at depths of 0~-21 m during the years 2001, 2002, 2003, 2004, 2005, and 2006 are plotted in Figure 12, respectively. The influence depths of climate conditions on soil volumetric water content vary slightly for different years: 4.0 m for the year 2001 (Figure 12a), 4.8 m for the year 2002 (Figure 12b), 6.0 m for the year 2003 (Figure 12c), 3.2 m for year 2004 (Figure 12d), 8.0 m for year 2005 (Figure 12e) and 10 m for year 2006 (Figure 12f). Among the studied period, the influence depth in terms of soil water content presents the largest and smallest values in the years 2006 and 2004, respectively. However, more frequent rainfall events (Figure 4d) are recorded in the years 2003, 2004, 2005 and 2006. It infers that the relationship between the influence depth and the changing climate conditions is not significant as expected. This may be attributed to that the value of net water flux conditions is governed by both rainfall and evaporation on the soil surface.

On the other hand, the soil temperature profiles in different years (2000 to 2006) at depths of 0~-21 m are shown in Figure 13, presenting the influence depths of climate conditions: 18.4 m in the year 2001 (Figure 13a), smaller than 20 m in other years (Figures 13b~f). The influence depth of climate conditions on temperature increases as time continues. It is inferred to be related to the

323 warming climate conditions produced by the increasing solar radiation from the year 2000 to the
324 year 2006 in Figure 7a.

325 As shown in Figures 12h and 13h, in the studied period of seven years (2000 to 2006), the
326 influence depths of climate conditions are estimated to be larger than 20 m for both soil water
327 content and temperature. It indicates that the overburden and the current storage space for
328 LLW/ILW are potentially situated in the weather influenced zone in the future. Therefore, further
329 investigation about the effect of soil water content and temperature on the performance of
330 LLW/ILW storage system is required to minimize the negative weather influence on LLW/ILW
331 storage and to provide a practical suggestion for future site selections. Based on the results of each
332 year and seven years, it is inferred that the influence depths of climate conditions vary significantly
333 in different studied periods. The differences are governed by the climate conditions of the studied
334 periods. During the longer studied period (7 years), the influence of climate conditions on the
335 variations of soil volumetric water content and temperature is accumulated, leading to a deeper
336 influenced zone compared to that of each year. It may be attributed to the effect of wetting-drying
337 cycles during the longer period on the changes of soil microstructure, allowing heat and water
338 transport to a deeper zone.

339

340 **5. Conclusions**

341 In this study, the effect of climate conditions on soil water content and temperature in the
342 overburden of LLW/ILW disposal facility were numerically investigated at different time scales
343 (30 min, daily, weekly and monthly) and in the long term (7 years). Actual meteorological
344 information data from Valencia El Saler station in Spain were used as the future climate conditions

of the studied site in middle France based on climate analogues. The obtained results allow the following conclusions to be drawn:

(1) The variations of soil volumetric water content and temperature in the near-surface zone are mainly affected by the hydraulic (evaporation/infiltration) and thermal (soil heat flux) boundary conditions at the soil-atmosphere interface. At soil surface, distinct daily and seasonal variations of soil temperature can be observed, with higher values during the summer period and lower values in the wintertime. In the deeper zone, both soil volumetric water content and temperature show much smaller fluctuations compared to those of near soil surface zone.

(2) The calculated results in terms of soil volumetric water content and temperature present a similar variation tendency at the same depth for the four different time scales. However, in general, the results at the time scale of 30 min depict the maximum and minimum values because of the extreme climate events recorded at this time interval. The daily fluctuations of soil water content and temperature are more evident at the time scale of 30 min than those of other time scales, especially at soil surface point. As a result, the employment of meteorological information at a short time scale (30 min) can increase the accuracy of simulation results by capturing the extreme climate events and accelerating the iteration rate of soil-atmosphere interaction. Thereby, it is suggested to apply the meteorological information at a short time scale (30 min) to estimate the soil hydro-thermal behavior in the geotechnical and environmental contexts.

(3) In terms of influence depth for soil water content in the year 2000, it is limited to 4.8 m, 5.2 m, 11.6 m, and 11.6 at the time scale of 30 min, daily, weekly, and monthly, respectively. The mass transfer between soil and atmosphere at the time scale of 30 min is more effective

than others. However, the influence depth in terms of soil temperature is limited to 12.0~12.8 m, indicating the insignificant effect of time scale. It may result from the same amount of energy transfer between soil and atmosphere at different time scales. Additional work is required to further clarify this point.

(4) The change of soil temperature in the long term (7 years) indicates that the peak temperatures of the summer periods show an increasing trend from 01/01/2000 to 31/12/2006, reflecting the effect of the warming climate on soil temperature. Moreover, the influence of climate conditions on soil hydro-thermal behavior is accumulated over time, leading to a deeper influenced zone (> 20 m) in a longer studied period. It indicates that the overburden and the current storage space for LLW/ILW are potentially situated in the weather influenced zone in the future.

(5) This study infers that a further investigation about the effect of soil water content and temperature variations on the performance of LLW/ILW storage system is required. It also enables a further detailed inspection of climate's role in the LLW/ILW storage system to minimize the negative influence of climate change on LLW/ILW storage and to provide a practical suggestion for site selections.

Acknowledgments

The authors wish to acknowledge the support from ANDRA (Agence Nationale pour la Gestion des Déchets Radioactifs) and Ecole des Ponts ParisTech (ENPC). The authors would also like to express their gratitude to Mr. Arnaud Carrara in Fundación Centro de Estudios Ambientales del Mediterráneo (CEAM) for collecting and providing the meteorological data at Valencia El Saler station in Spain.

References

[1] Giusti L. A review of waste management practices and their impact on human health. Waste Manag 2009;29:2227–39. https://doi.org/10.1016/j.wasman.2009.03.028.

[2] McCartney JS, Sánchez M, Tomac I. Energy geotechnics: Advances in subsurface energy recovery, storage, exchange, and waste management. Comput Geotech 2016;75:244–56. https://doi.org/10.1016/j.compgeo.2016.01.002.

[3] Zhang Y, Zhang QY, Duan K, Yu GY, Jiao YY. Reliability analysis of deep underground research laboratory in Beishan for geological disposal of high-level radioactive waste. Comput Geotech 2020;118:103328. https://doi.org/10.1016/j.compgeo.2019.103328.

[4] Yim MS, Simonson SA. Performance assessment models for low level radioactive waste disposal facilities: a review. Prog Nucl Energy 2000;36:1–38. https://doi.org/10.1016/S0149-1970(99)00015-3.

[5] Kim MS, Jeon JS, Kim MJ, Lee J, Lee SR. A multi-objective optimization of initial conditions in a radioactive waste repository by numerical thermo-hydro-mechanical modeling. Comput Geotech 2019;114:103106. https://doi.org/10.1016/j.compgeo.2019.103106.

[6] Näslund JO, Brandefelt J, Liljedahl LC. Climate considerations in long-term safety assessments for nuclear waste repositories. Ambio 2013;42:393–401. https://doi.org/10.1007/s13280-013-0406-6.

[7] Vardon PJ. Climatic influence on geotechnical infrastructure: A review. Environ Geotech 2015;2:166–74. https://doi.org/10.1680/envgeo.13.00055.

[8] Blight GE. Interactions between the atmosphere and the Earth. Géotechnique 1997;47:715–67. https://doi.org/10.1680/geot.1997.47.4.713.

[9] Cui YJ, Ta AN, Hemmati S, Tang AM, Gatmiri B. Experimental and numerical investigation of soil-atmosphere interaction. Eng Geol 2013;165:20–8. https://doi.org/10.1016/j.enggeo.2012.03.018.

[10] An N, Hemmati S, Cui Y. Numerical analysis of soil volumetric water content and temperature variations in an embankment due to soil-atmosphere interaction. Comput Geotech 2017;83:40–51. https://doi.org/10.1016/j.compgeo.2016.10.010.

[11] Craig RG. Evaluating the risk of climate change to nuclear waste disposal. Math Geol 1988;20:567–88. https://doi.org/10.1007/BF00890337.

[12] van Geet M, de Craen M, Beerten K, Leterme B, Mallants D, Wouters L, et al. Climate evolution in the long-term safety assessment of surface and geological disposal facilities for radioactive waste in Belgium. Geol Belgica 2012;15:8–15.

[13] Fischer JN. Hydrogeologic factors in the selection of shallow land burial sites for the disposal of low-level radioactive waste. US Geol Surv Circ 1986;973:22. https://doi.org/10.3133/cir973.

[14] Fischer JM. Sediment properties and water movement through shallow unsaturated alluvium at an arid site for disposal of low-level eadioactive qaste near beatty, Nye County, Nevada. 1992.

[15] Phillips DH, Sinnathamby G, Russell MI, Anderson C, Paksy A. Mineralogy of selected geological deposits from the United Kingdom and the Republic of Ireland as possible capping material for low-level radioactive waste disposal facilities. Appl Clay Sci 2011;53:395–401. https://doi.org/10.1016/j.clay.2010.05.006.

[16] Nasir O, Fall M, Evgin E. A simulator for modeling of porosity and permeability changes in near field sedimentary host rocks for nuclear waste under climate change influences. Tunn Undergr Sp Technol 2014;42:122–35. https://doi.org/10.1016/j.tust.2014.02.010.

[17] Smith E. Natural physical and biological processes compromise the long-term integrity of compacted clay caps. Proc. DOE/National Acad. Sci. Work. Barriers Long Term Isol., Washington, DC: Denver, National Academy Press; 1997.

[18] Hecht F. FreeFem++, a tool to solve PDE's numerically. 2010.

[19] Plas F, Brulhet J, Conil N. Référentiel du site de la Communauté de Communes de Soulaines– Projet FAVL Communauté de Communes de Soulaines. Programme de reconnaissance, ANDRA report-F.NT.ADSD.13.0023. 2015.

[20] Mickley AS. The thermal conductivity of moist soil. Trans Am Inst Electr Eng 1951;70:1789–97. https://doi.org/10.1109/T-AIEE.1951.5060631.

[21] Pauly NM. Thermal conductivity of soils from the analysis of boring logs. Master Thesis, University of South Florida, 2010.

[22] Escario V, Juca J, Coppe M. Strength and deformation of partly saturated soils. Proc. 12th Int. Conf. Soil Mech. Found. Eng., Rio de Janerio, Brazil: 1989, p. 43–6.

[23] Jahangir MH, Sadrnejad SA. A new coupled heat, moisture and air transfer model in unsaturated soil. J Mech Sci Technol 2012;26:3661–72. https://doi.org/10.1007/s12206-012-0839-z.

[24] van Genuchten MT. Closed-Form Equation for Predicting the Hydraulic Conductivity of Unsaturated Soils. Soil Sci Soc Am J 1980;44:892–8. https://doi.org/10.2136/sssaj1980.03615995004400050002x.

[25] Swiss Standard SN 670 010b, Characteristic coefficients of soils n.d.

[26] Tang AM, Cui YJ, Le TT. A study on the thermal conductivity of compacted bentonites. Appl Clay Sci 2008;41:181–9. https://doi.org/10.1016/j.clay.2007.11.001.

[27] De Vries DA. Thermal properties of soils. In: Van Wijk WR, editor. Phys. plant Environ. (ed. W. R. Van Wijk), Amsterdam: North-Holland.: 1963, p. 210–235.

[28] Cui YJ, Lu YF, Delage P, Riffard M. Field simulation of in situ water content and temperature changes due to ground–atmospheric interactions. Géotechnique 2005;55:557–67. https://doi.org/10.1680/geot.2005.55.7.557.

[29] Cuisinier O, Masrouri F. Détermination des propriétés hydromécaniques des argiles tégulines et des marnes de Brienne – Projet FAVL Rapport final. 2015.

[30] Zhang F, Cui Y-J, Zeng L, Conil N. Anisotropic features of natural Teguline clay. Eng Geol 2019;261:105275. https://doi.org/10.1016/j.enggeo.2019.105275.

[31] Zeng LL, Cui YJ, Conil N, Zghondi J, Armand G, Talandier J. Experimental study on swelling behaviour and microstructure changes of natural stiff teguline clays upon wetting. Can Geotech J 2017;54:700–9. https://doi.org/10.1139/cgj-2016-0250.

[32] Hallegatte S, Hourcade JC, Ambrosi P. Using climate analogues for assessing climate change economic impacts in urban areas. Clim Change 2007;82:47–60. https://doi.org/10.1007/s10584-006-9161-z.

[33] Kopf S, Ha-Duong M, Hallegatte S. Using maps of city analogues to display and interpret climate change scenarios and their uncertainty. Nat Hazards Earth Syst Sci 2008;8:905–18. https://doi.org/10.5194/nhess-8-905-2008.

[34] Beck HE, Zimmermann NE, McVicar TR, Vergopolan N, Berg A, Wood EF. Present and future köppen-geiger climate classification maps at 1-km resolution. Sci Data 2018;5:1–12. https://doi.org/10.1038/sdata.2018.214.

[35] An N, Hemmati S, Cui Y, Mercadier D. Assessment of Rainfall Runoff Based on the Field Measurements on an Embankment. Geotech Test J 2017;40:20160096. https://doi.org/10.1520/GTJ20160096.

Table captions

Table 1. Soil properties of each layer in the study region

Table 2. Soil thermal conductivity, water retention curve and hydraulic conductivity curve of each layer in the study region

Figure captions

Figure 1. (a) Schematic diagram of the studied region and (b) detailed soil information of different layers

Figure 2. Soil properties of three layers: (a) the variations of soil thermal conductivity versus volumetric water content; (b) the variations of soil water retention versus suction, and (c) the variations of soil hydraulic conductivity versus suction

Figure 3. Field meteorological information recorded from 01/01/2000 to 31/12/2000 at different time scales (30 min, daily, weekly and monthly): (a) solar radiation, (b) air temperature, (c) latent heat, (d) rainfall and (e) actual evaporation rate (calculated)

Figure 4. Field meteorological information from 01/01/2000 to 31/12/2006 at the time scales of 30 min: (a) solar radiation, (b) air temperature, (c) latent heat, (d) rainfall and (e) actual evaporation rate (calculated)

Figure 5. Numerical model dimensions used in this study

Figure 6. At the time scale of 30 min: the variations of (a) soil volumetric water content and (b) soil temperature at depths of 0 m, -0.25 m, -0.5 m, -0.75 m, -1.0 m, and -1.5 m during the studied period

Figure 7. At the time scale of 30 min: (a) soil volumetric water content profiles and (b) temperature profiles at different times in zone 0~-20 m

523 Figure 8. Soil volumetric water content variations at different time scales (30 min, daily, weekly
524 and monthly) at depths of (a) 0 m, (b) -0.25, (c) -0.75 m, and (d) -1.5 m
525 Figure 9. Soil temperature variations at different time scales (30 min, daily, weekly and monthly)
526 at depths of (a) 0 m, (b) -0.25, (c) -0.75 m, and (d) -1.5 m
527 Figure 10. Soil volumetric water content and temperature profiles in zone 0~-20 m during the year
528 2000 at different time scales: (a) daily; (b) weekly, and (c) monthly
529 Figure 11. At the time scale of 30 min, the variations of soil (a) volumetric water content and (b)
530 temperature at depths of 0 m, -0.25, -0.5 m, -0.75 m, -1.0 m, and -1.5 m from 01/01/2000 to
531 31/12/2006
532 Figure 12. At the time scale of 30 min, soil volumetric water content profiles at different times in
533 zone 0~-20 m during different studied periods: (a) year 2001, (b) year 2002, (c) year 2003, (d) year
534 2004, (e) year 2005, (f) year 2006, and (g) from year 2000 to 2006
535 Figure 13. At the time scale of 30 min, soil temperature profiles at different times in zone 0~-20 m
536 during different studied periods: (a) year 2001, (b) year 2002, (c) year 2003, (d) year 2004, (e) year
537 2005, (f) year 2006, and (g) from year 2000 to 2006
538
539
540
541
542
543
544
545
546
547
548
549
550

Tables

Table 1. Soil properties of each layer in the study region

Layer	Soil	Depth (m)	Porosity	Dry density (Mg/m^3)
L1	Silty clay	0~-1	0.35	1.3
L2	Compacted Teguline clay	-1~-36	0.37	1.7
L3	Natural Teguline clay	-36~-71	0.256	2.0

Table 2. Soil thermal conductivity, water retention curve and hydraulic conductivity curve of each layer in the study region

Layer	Soil thermal conductivity	Soil water retention curve		Soil hydraulic conductivity curve		
		$S_e = \frac{\theta - \theta_r}{\theta_s - \theta_r} = \left[1 + (\alpha\psi)^n\right]^{-m}$ (2)		$K = K_s S_e^{0.5}\left[1 - \left(1 - S_e^{1/m}\right)^m\right]^2$ (3)		
		θ_s	θ_r	α	n	K_s
L1	$\lambda = 1.55\theta + 0.47$ (1)	0.32	0.00	0.0285	1.627	1.0×10^{-8}
L2	$\lambda = 4.53\theta + 0.15$ (4)	0.37	0.004	3.5×10^{-4}	1.60	1.4×10^{-9}
L3	$\lambda = 2.0$	0.245	0.004	8.0×10^{-5}	1.80	3.0×10^{-12}

Comments: λ (W/(m·K)) is soil thermal conductivity;
θ is soil volumetric water content;
S_e is soil effective saturation;
θ_s is saturated volumetric water content;
θ_r is residual volumetric water content;
α (kPa^{-1}), m and n are soil constants, $m = 1-1/n$;
K (m/s) is soil hydraulic conductivity;
K_s (m/s) is soil saturated hydraulic conductivity.

Figures

(a)

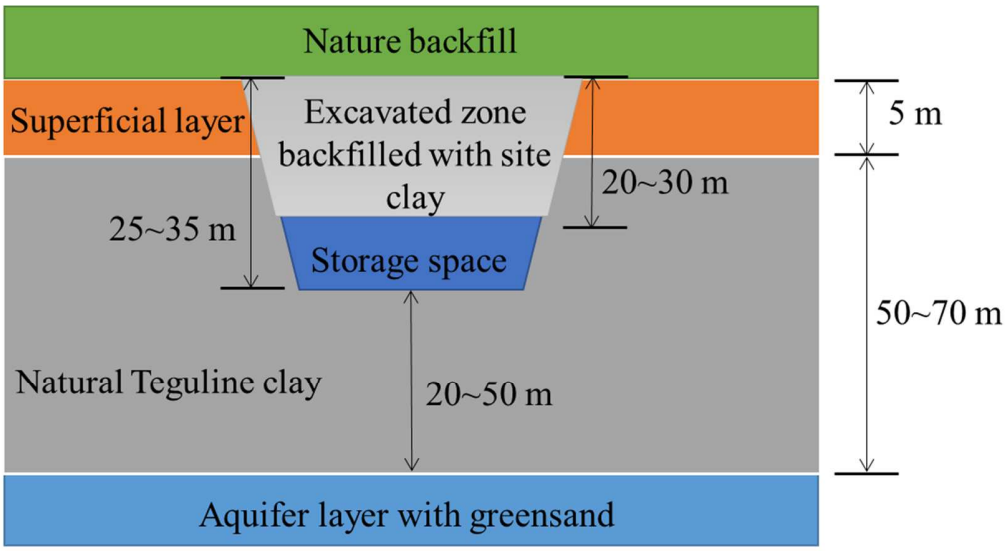

(b)

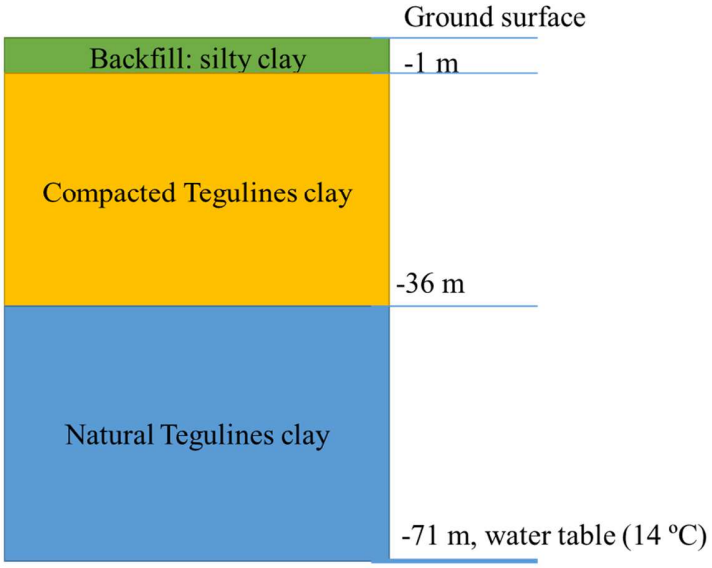

Figure 1. (a) Schematic diagram of the studied region and (b) detailed soil information of different layers

(a)

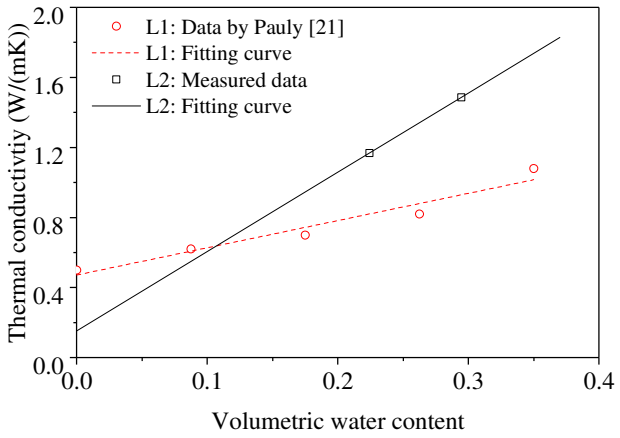

(b)

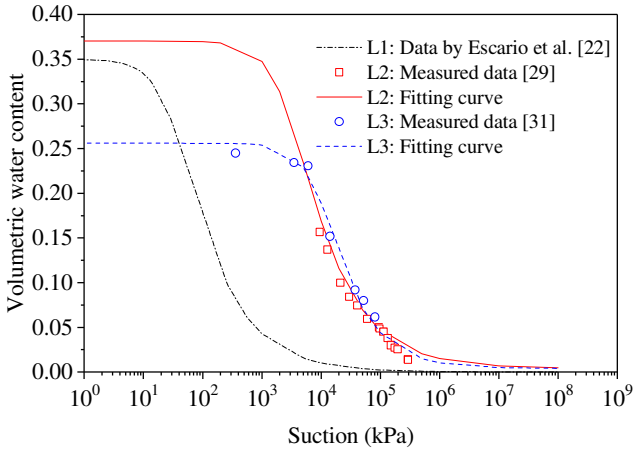

(c)

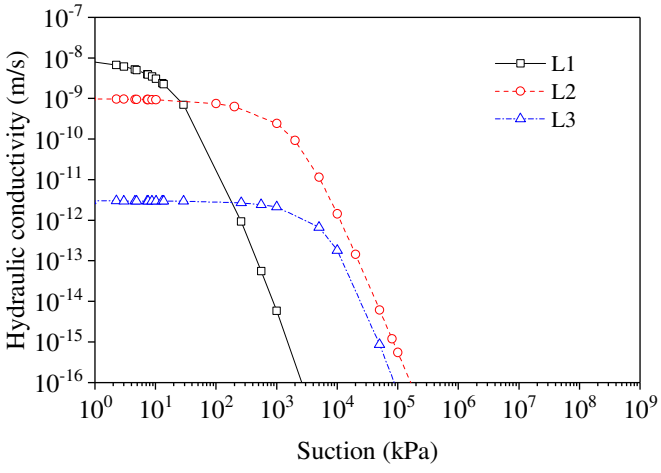

618 Figure 2. Soil properties of three layers: (a) the variations of soil thermal conductivity versus
619 volumetric water content; (b) the variations of soil water retention versus suction, and (c) the
620 variations of soil hydraulic conductivity versus suction

621

(a)

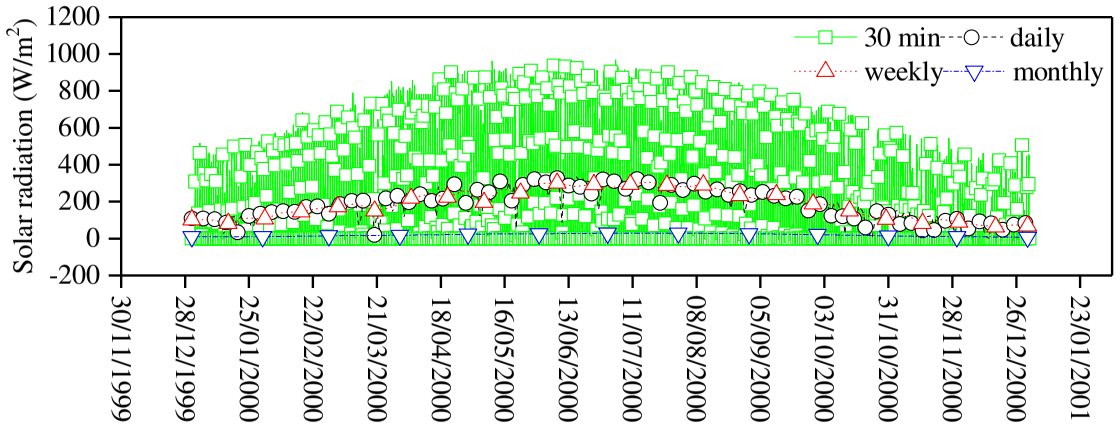
Solar radiation (W/m2)
1200
1000
800
600
400
200
0
-200
30 min
daily
weekly
monthly
30/11/1999
28/12/1999
25/01/2000
22/02/2000
21/03/2000
18/04/2000
16/05/2000
13/06/2000
11/07/2000
08/08/2000
05/09/2000
03/10/2000
31/10/2000
28/11/2000
26/12/2000
23/01/2001

(b)

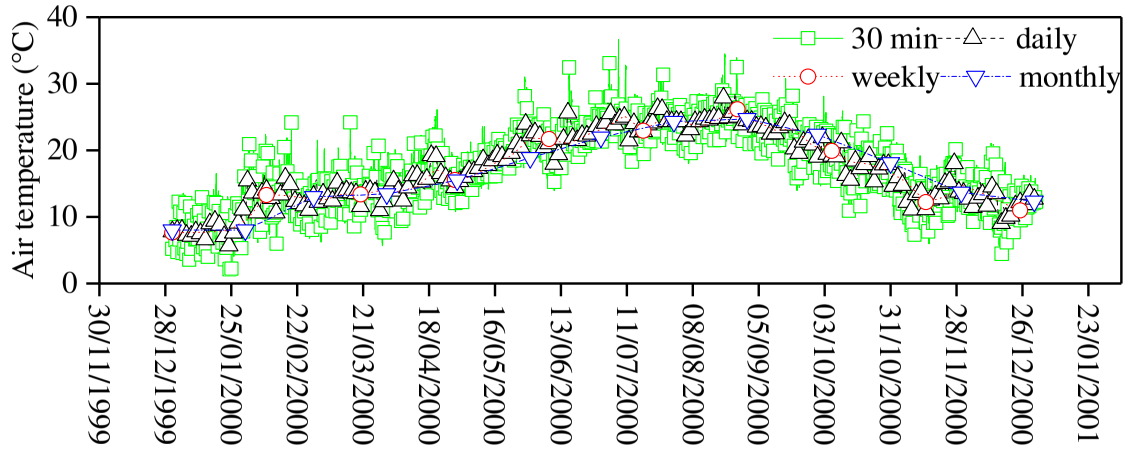
Air temperature (°C)
40
30
20
10
0
30 min
daily
weekly
monthly
30/11/1999
28/12/1999
25/01/2000
22/02/2000
21/03/2000
18/04/2000
16/05/2000
13/06/2000
11/07/2000
08/08/2000
05/09/2000
03/10/2000
31/10/2000
28/11/2000
26/12/2000
23/01/2001

(c)

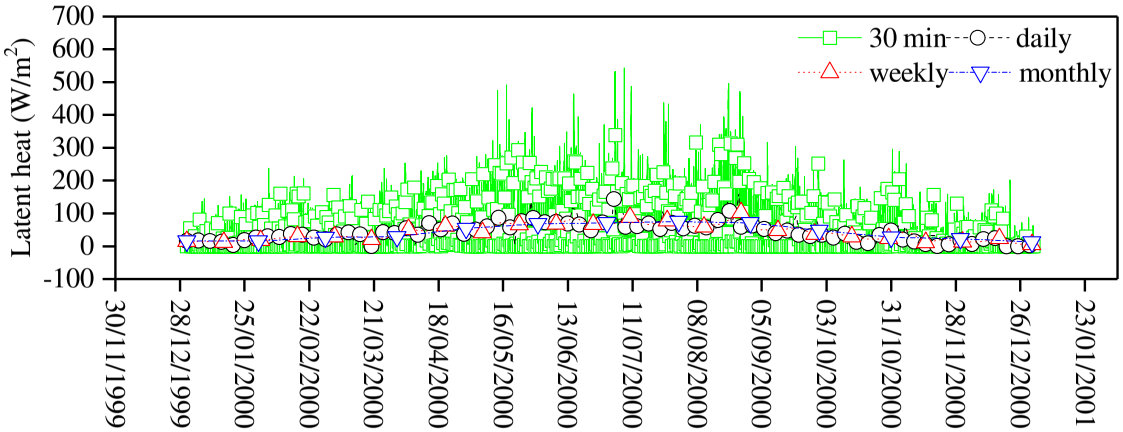
Latent heat (W/m2)
700
600
500
400
300
200
100
0
-100
30 min
daily
weekly
monthly
30/11/1999
28/12/1999
25/01/2000
22/02/2000
21/03/2000
18/04/2000
16/05/2000
13/06/2000
11/07/2000
08/08/2000
05/09/2000
03/10/2000
31/10/2000
28/11/2000
26/12/2000
23/01/2001

(d)

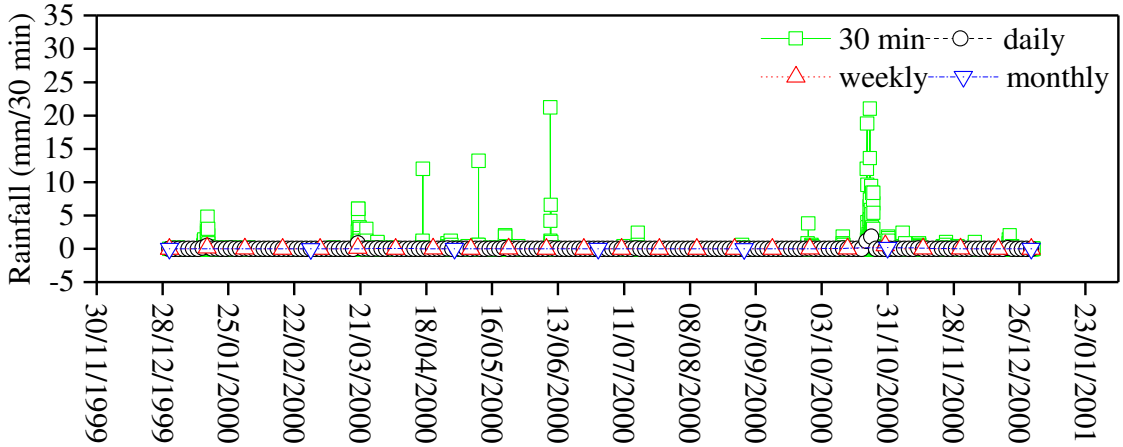

(e)

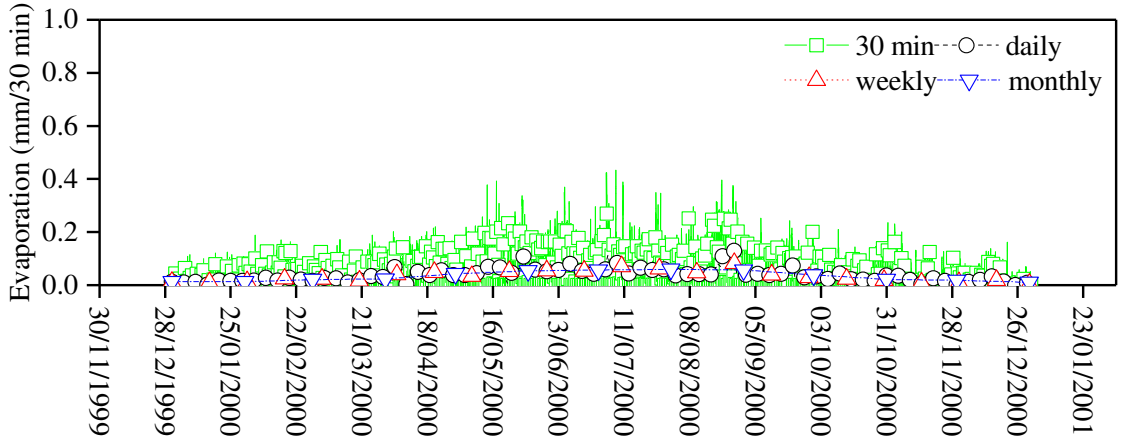

622

623 Figure 3. Field meteorological information recorded from 01/01/2000 to 31/12/2000 at different
624 time scales (30 min, daily, weekly and monthly): (a) solar radiation, (b) air temperature, (c) latent
625 heat, (d) rainfall and (e) actual evaporation rate (calculated)

626

627

628

629

630

631

(a)

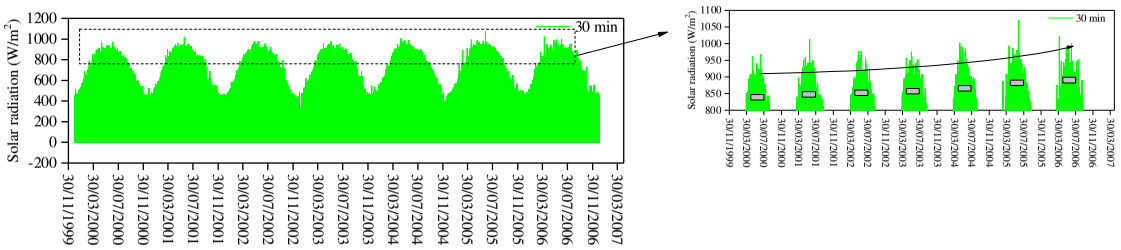
Solar radiation (W/m²)
30 min

(b)

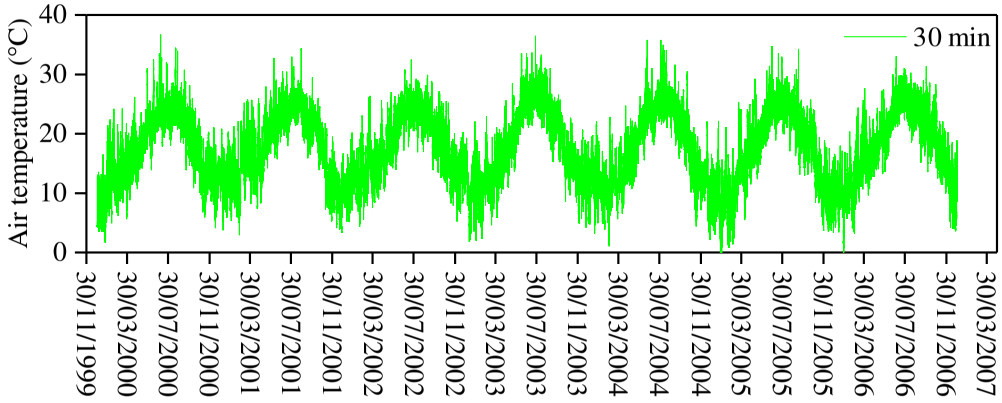
Air temperature (°C)
30 min

(c)

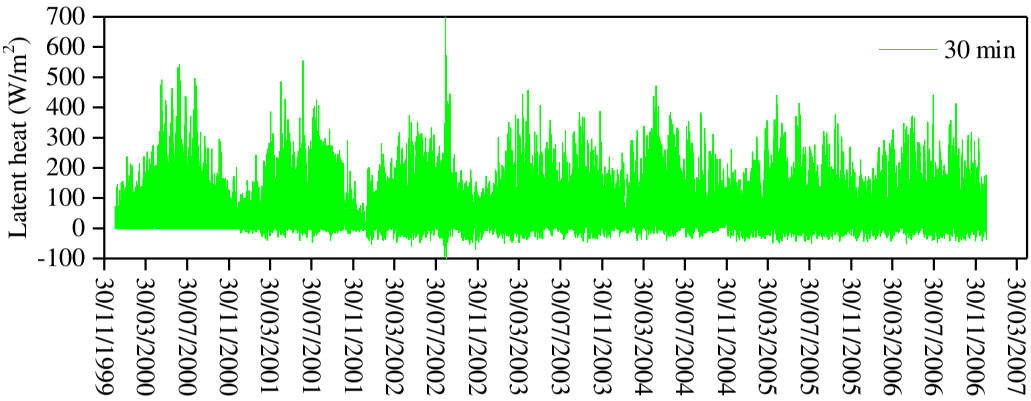
Latent heat (W/m²)
30 min

(d)

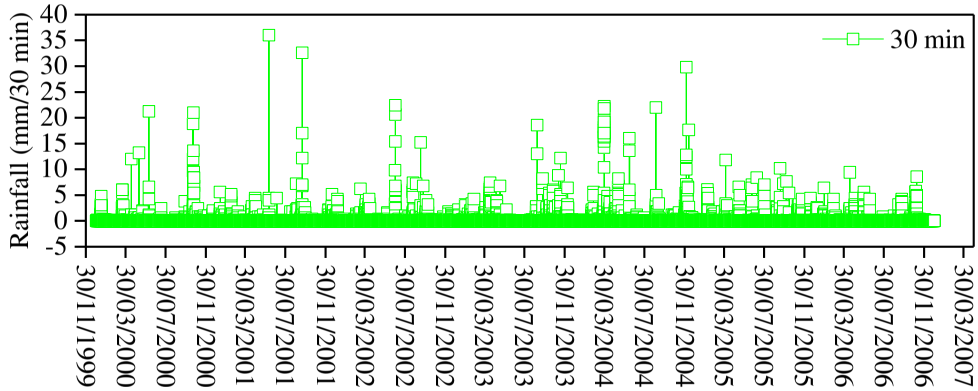
Rainfall (mm/30 min)
30 min

(e)

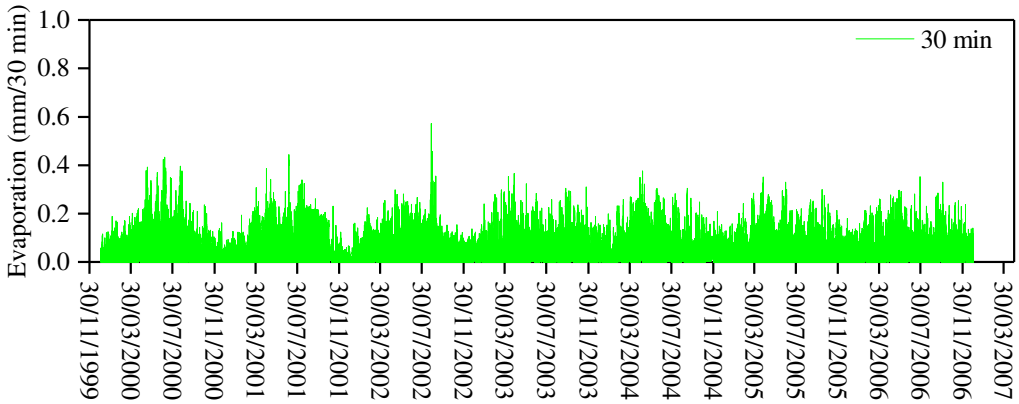

Figure 4. Field meteorological information from 01/01/2000 to 31/12/2006 at the time scales of 30 min: (a) solar radiation, (b) air temperature, (c) latent heat, (d) rainfall and (e) actual evaporation rate (calculated)

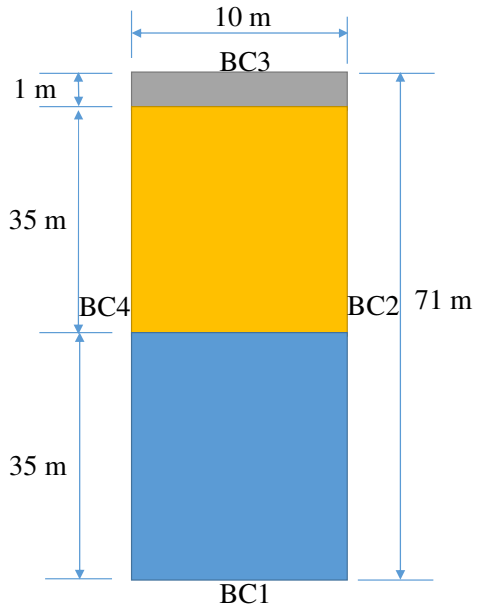

644

645 Figure 5. Numerical model dimensions used in this study

646

647

648

649

650

651

652

653

654

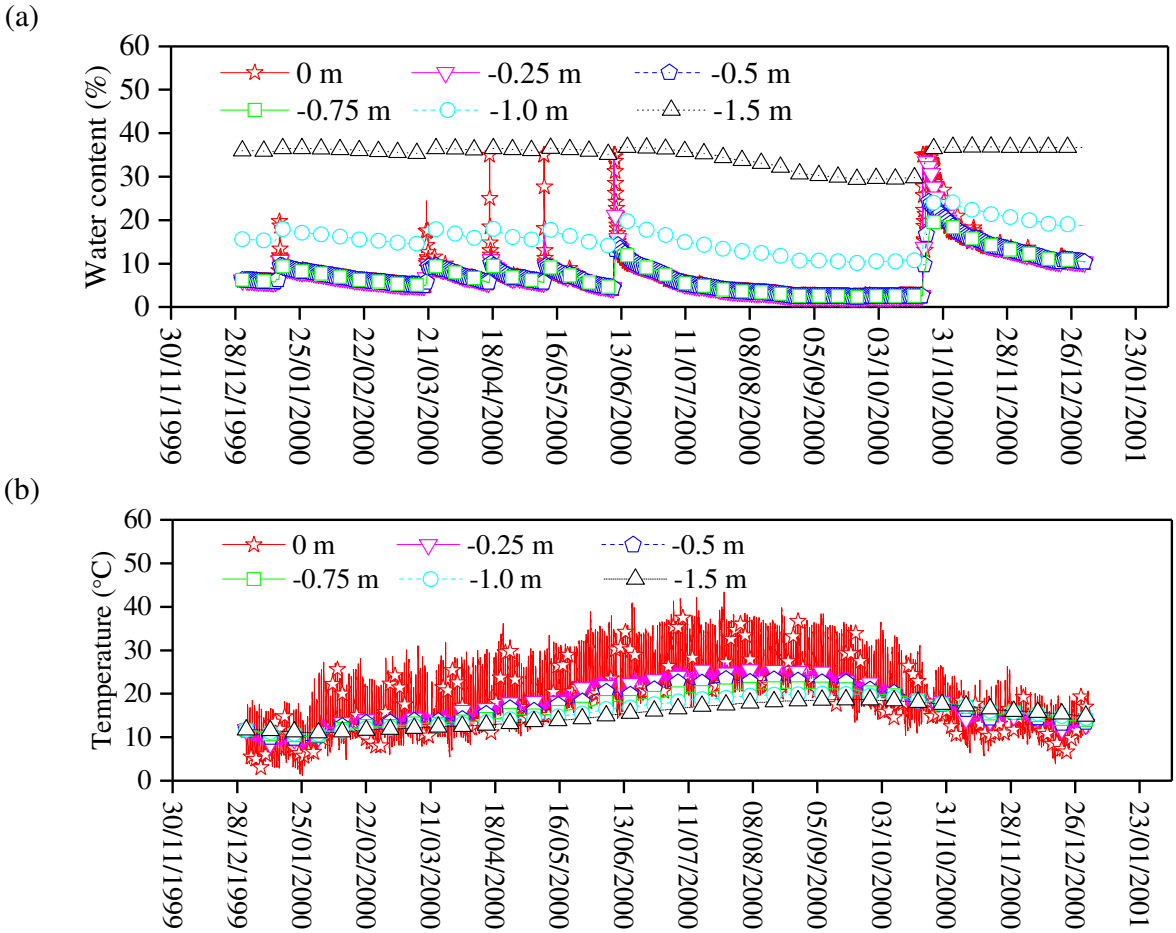

Figure 6. At the time scale of 30 min: the variations of (a) soil volumetric water content and (b) soil temperature at depths of 0 m, -0.25 m, -0.5 m, -0.75 m, -1.0 m, and -1.5 m during the studied period

(a)

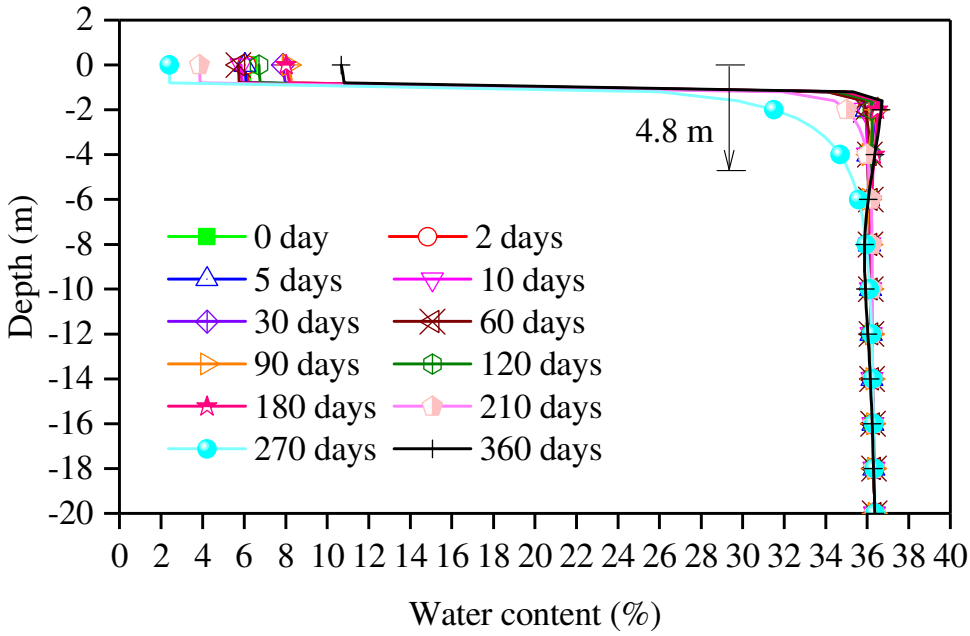

(b)

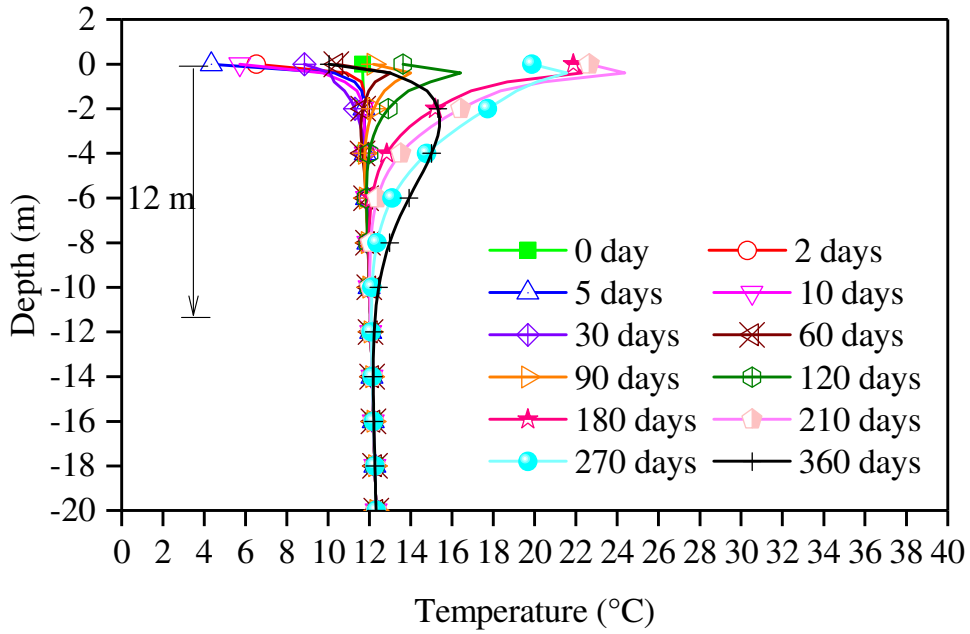

662

663 Figure 7. At the time scale of 30 min: (a) soil volumetric water content profiles and (b) temperature
664 profiles at different times in zone 0~-20 m

665

666

667

(a)

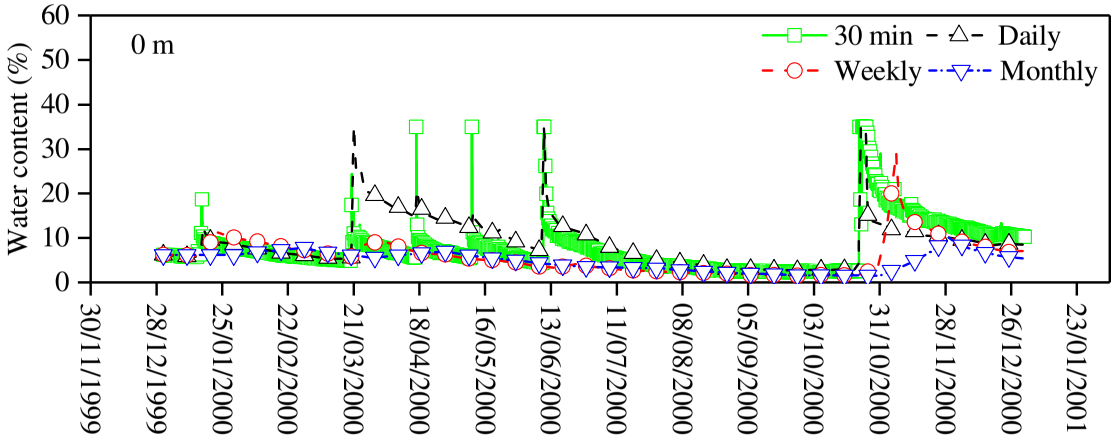
0 m
30 min
Daily
Weekly
Monthly
Water content (%)
0
10
20
30
40
50
60
30/11/1999
28/12/1999
25/01/2000
22/02/2000
21/03/2000
18/04/2000
16/05/2000
13/06/2000
11/07/2000
08/08/2000
05/09/2000
03/10/2000
31/10/2000
28/11/2000
26/12/2000
23/01/2001

(b)

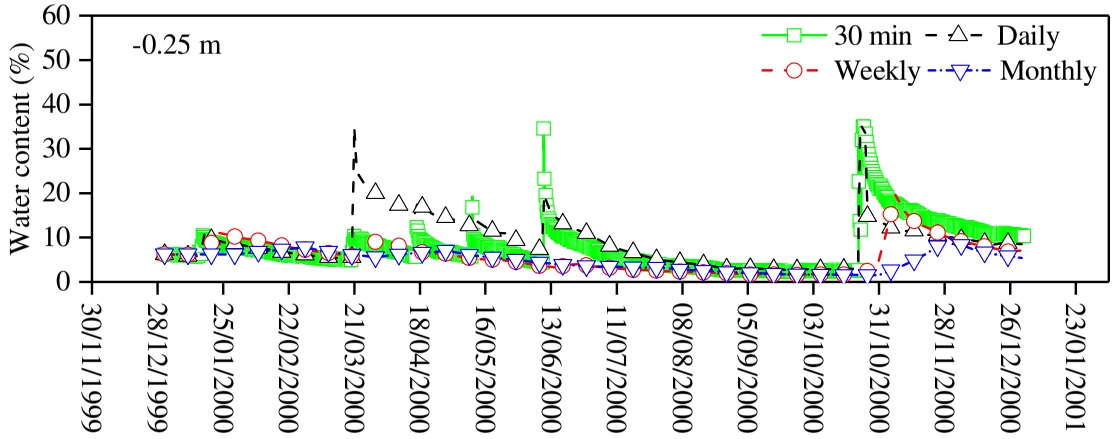
-0.25 m
30 min
Daily
Weekly
Monthly
Water content (%)
0
10
20
30
40
50
60
30/11/1999
28/12/1999
25/01/2000
22/02/2000
21/03/2000
18/04/2000
16/05/2000
13/06/2000
11/07/2000
08/08/2000
05/09/2000
03/10/2000
31/10/2000
28/11/2000
26/12/2000
23/01/2001

(c)

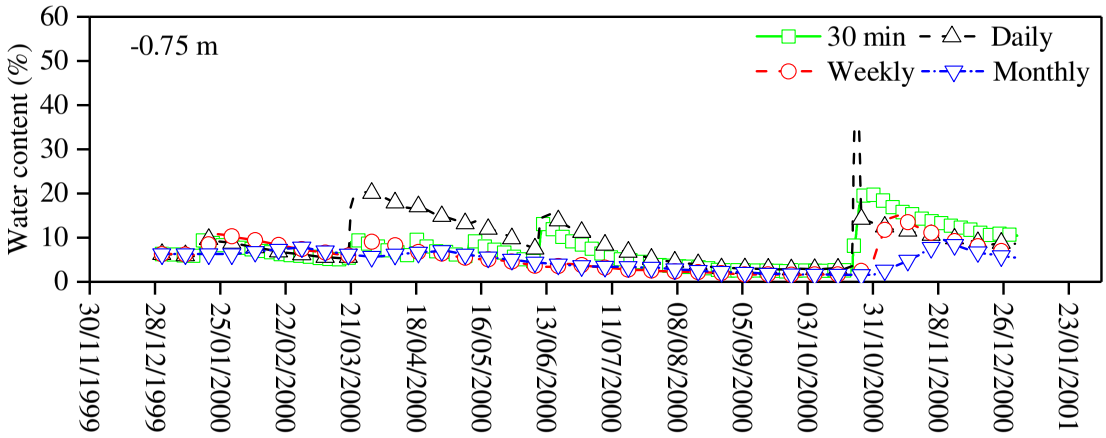
-0.75 m
30 min
Daily
Weekly
Monthly
Water content (%)
0
10
20
30
40
50
60
30/11/1999
28/12/1999
25/01/2000
22/02/2000
21/03/2000
18/04/2000
16/05/2000
13/06/2000
11/07/2000
08/08/2000
05/09/2000
03/10/2000
31/10/2000
28/11/2000
26/12/2000
23/01/2001

(d)

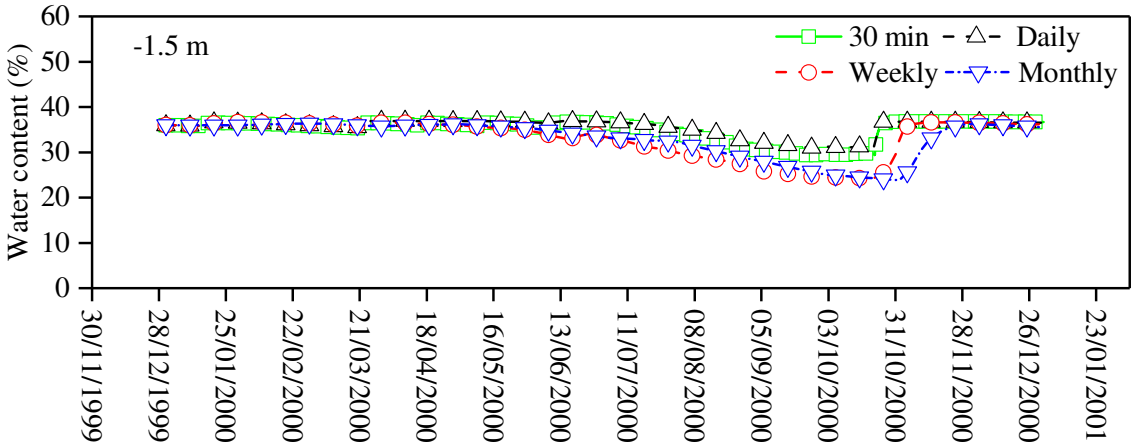

Figure 8. Soil volumetric water content variations at different time scales (30 min, daily, weekly and monthly) at depths of (a) 0 m, (b) -0.25, (c) -0.75 m, and (d) -1.5 m

(a)

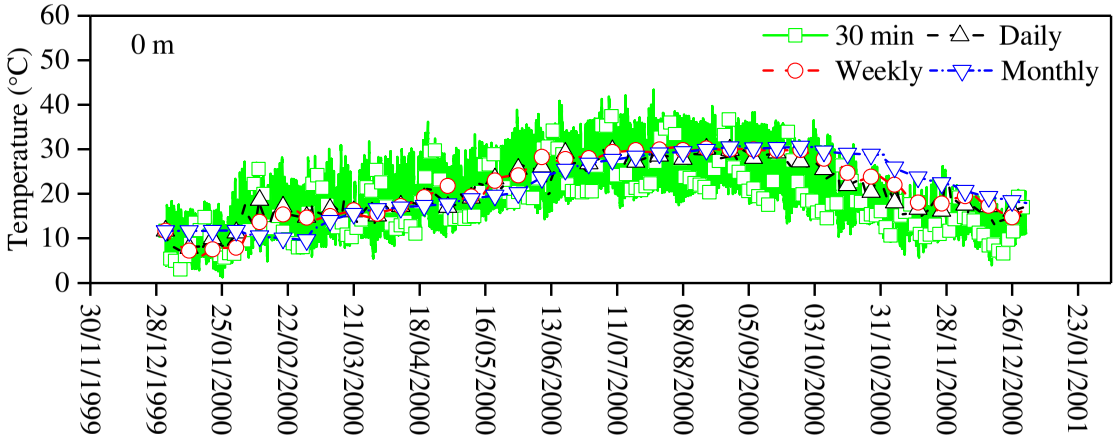
0 m
30 min
Daily
Weekly
Monthly
Temperature (°C)
0
10
20
30
40
50
60
30/11/1999
28/12/1999
25/01/2000
22/02/2000
21/03/2000
18/04/2000
16/05/2000
13/06/2000
11/07/2000
08/08/2000
05/09/2000
03/10/2000
31/10/2000
28/11/2000
26/12/2000
23/01/2001

(b)

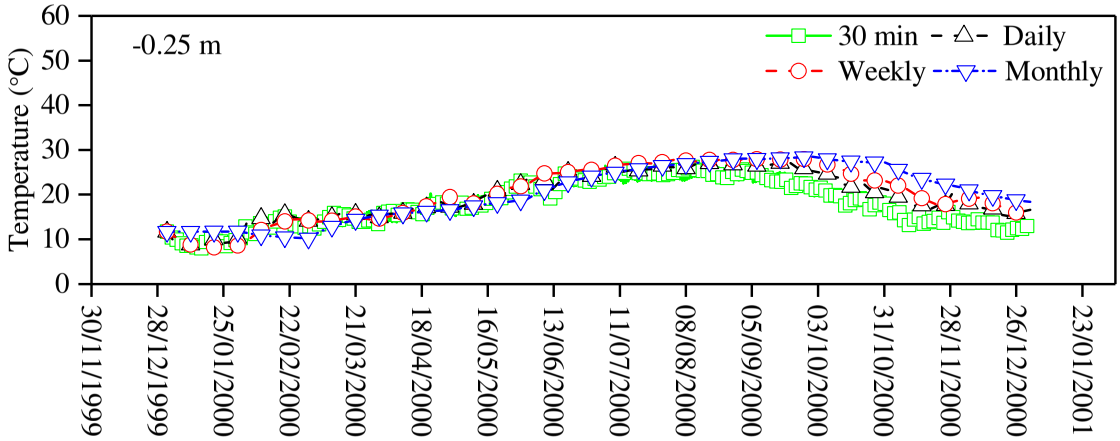
-0.25 m
30 min
Daily
Weekly
Monthly
Temperature (°C)
0
10
20
30
40
50
60
30/11/1999
28/12/1999
25/01/2000
22/02/2000
21/03/2000
18/04/2000
16/05/2000
13/06/2000
11/07/2000
08/08/2000
05/09/2000
03/10/2000
31/10/2000
28/11/2000
26/12/2000
23/01/2001

(c)

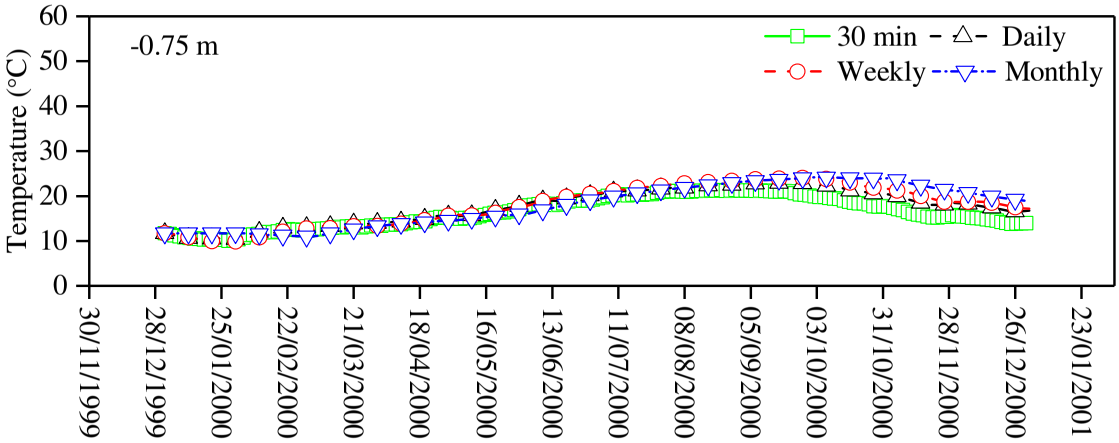
-0.75 m
30 min
Daily
Weekly
Monthly
Temperature (°C)
0
10
20
30
40
50
60
30/11/1999
28/12/1999
25/01/2000
22/02/2000
21/03/2000
18/04/2000
16/05/2000
13/06/2000
11/07/2000
08/08/2000
05/09/2000
03/10/2000
31/10/2000
28/11/2000
26/12/2000
23/01/2001

(d)

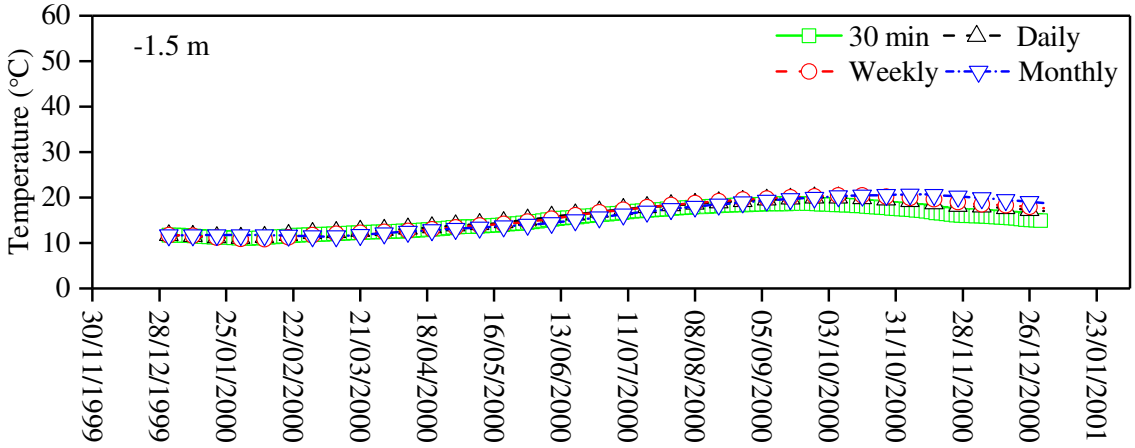

Figure 9. Soil temperature variations at different time scales (30 min, daily, weekly and monthly) at depths of (a) 0 m, (b) -0.25, (c) -0.75 m, and (d) -1.5 m

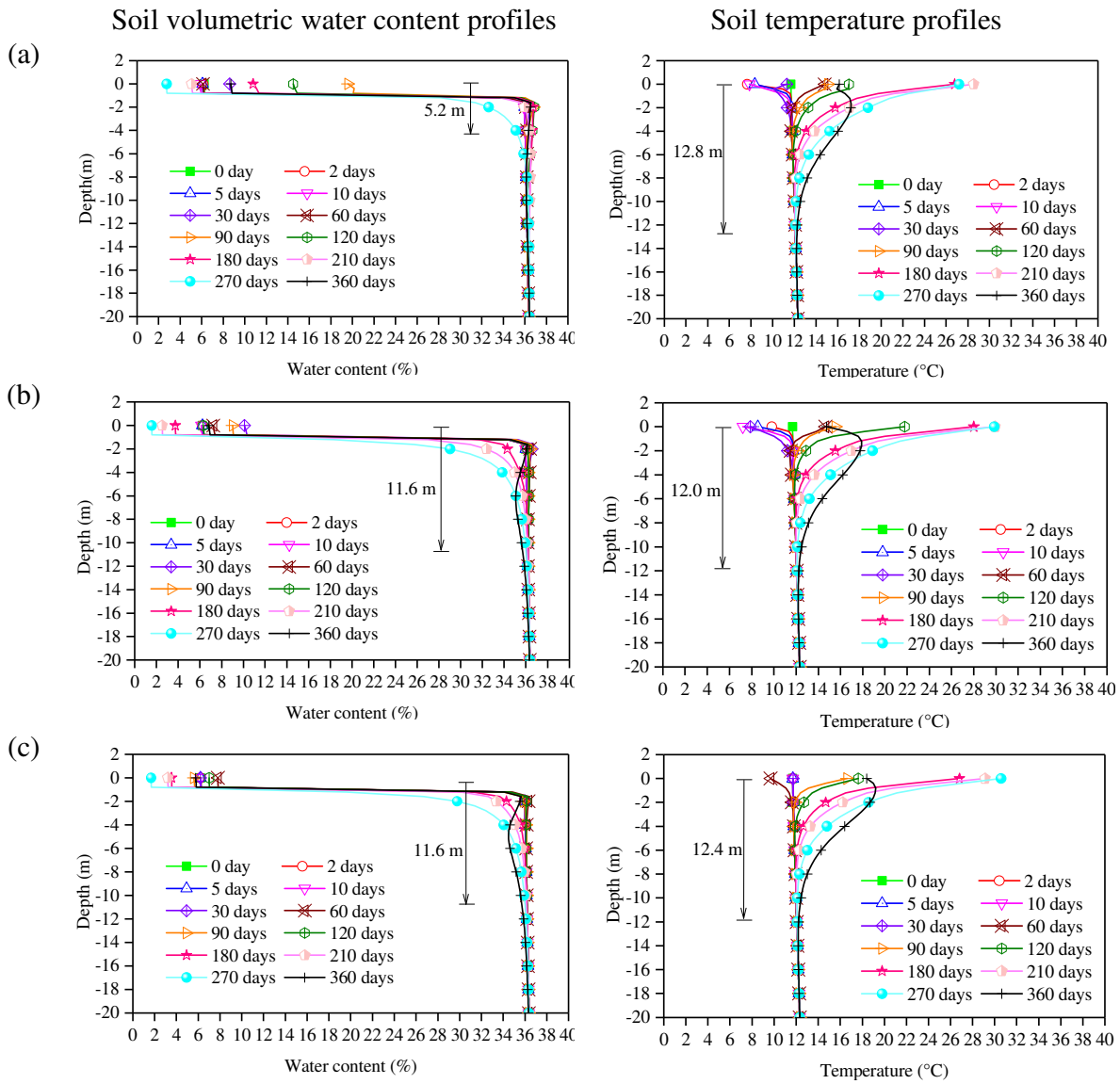

Figure 10. Soil volumetric water content and temperature profiles in zone 0~-20 m during the year 2000 at different time scales: (a) daily; (b) weekly, and (c) monthly

714

715

(a)

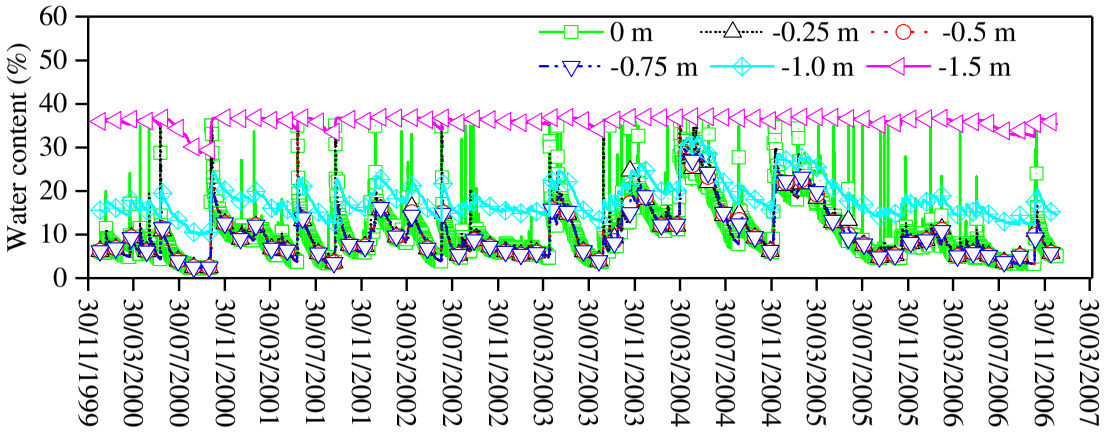

(b)

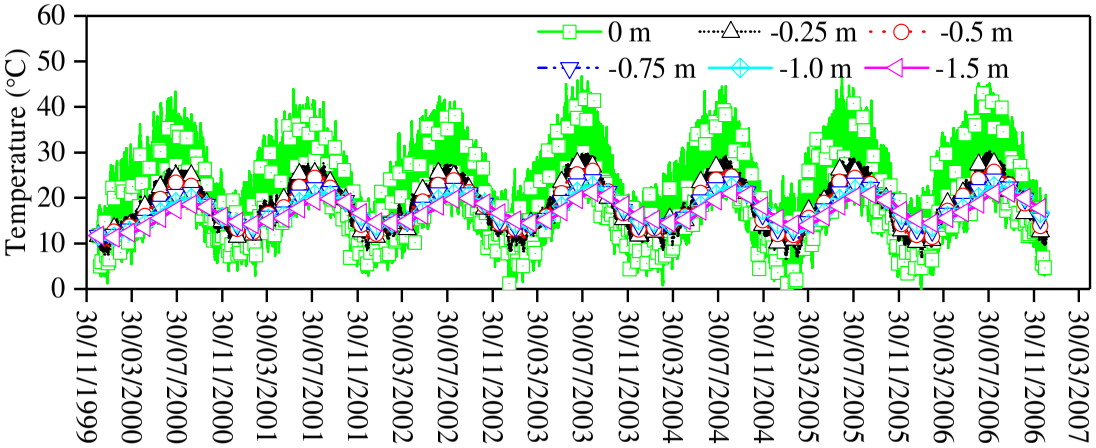

716

717 Figure 11. At the time scale of 30 min, the variations of soil (a) volumetric water content and (b)
718 temperature at depths of 0 m, -0.25, -0.5 m, -0.75 m, -1.0 m, and -1.5 m from 01/01/2000 to
719 31/12/2006

720

721

722

723

724

725

726

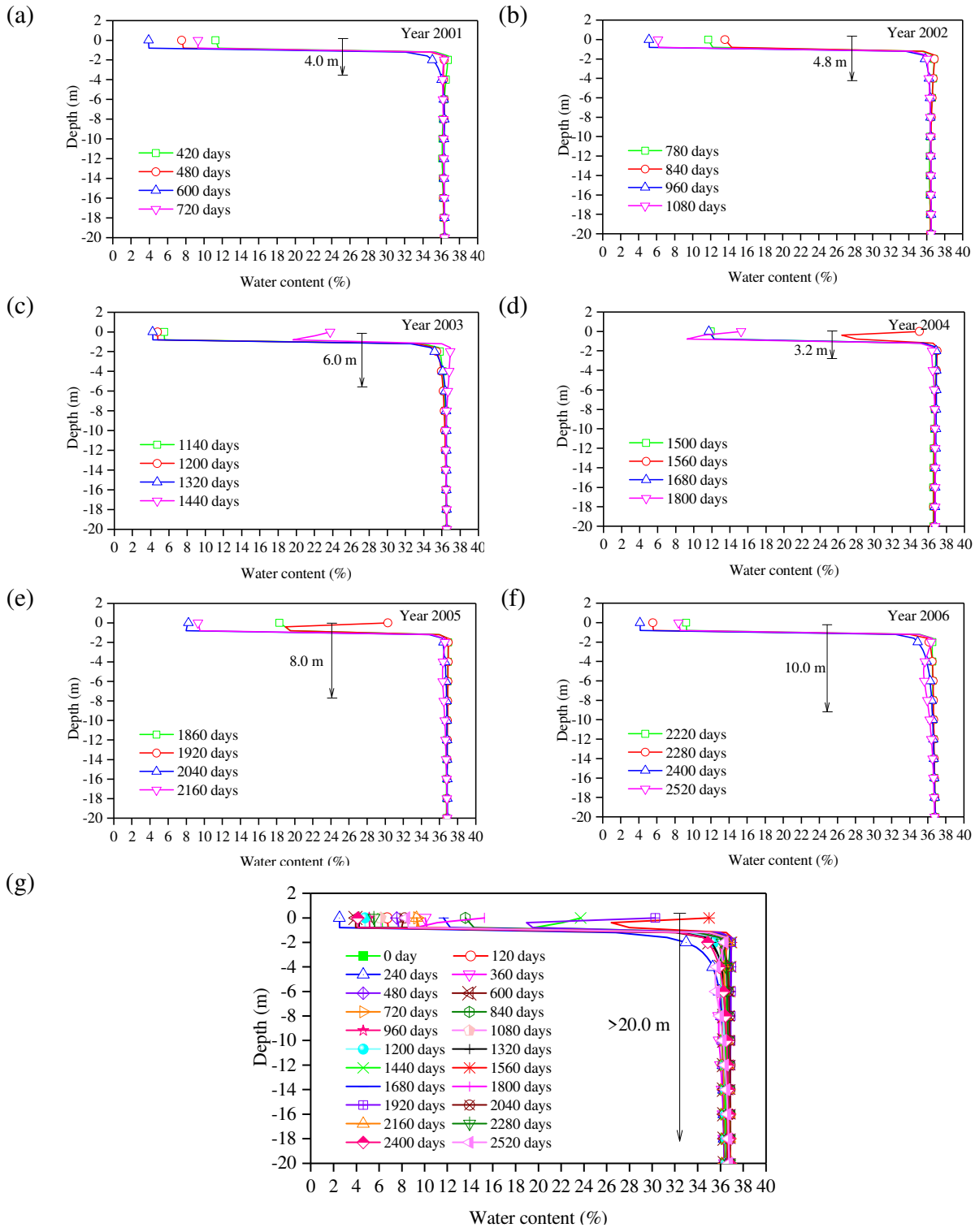

Figure 12. At the time scale of 30 min, soil volumetric water content profiles at different times in zone 0~-20 m during different studied periods: (a) year 2001, (b) year 2002, (c) year 2003, (d) year 2004, (e) year 2005, (f) year 2006, and (g) from year 2000 to 2006

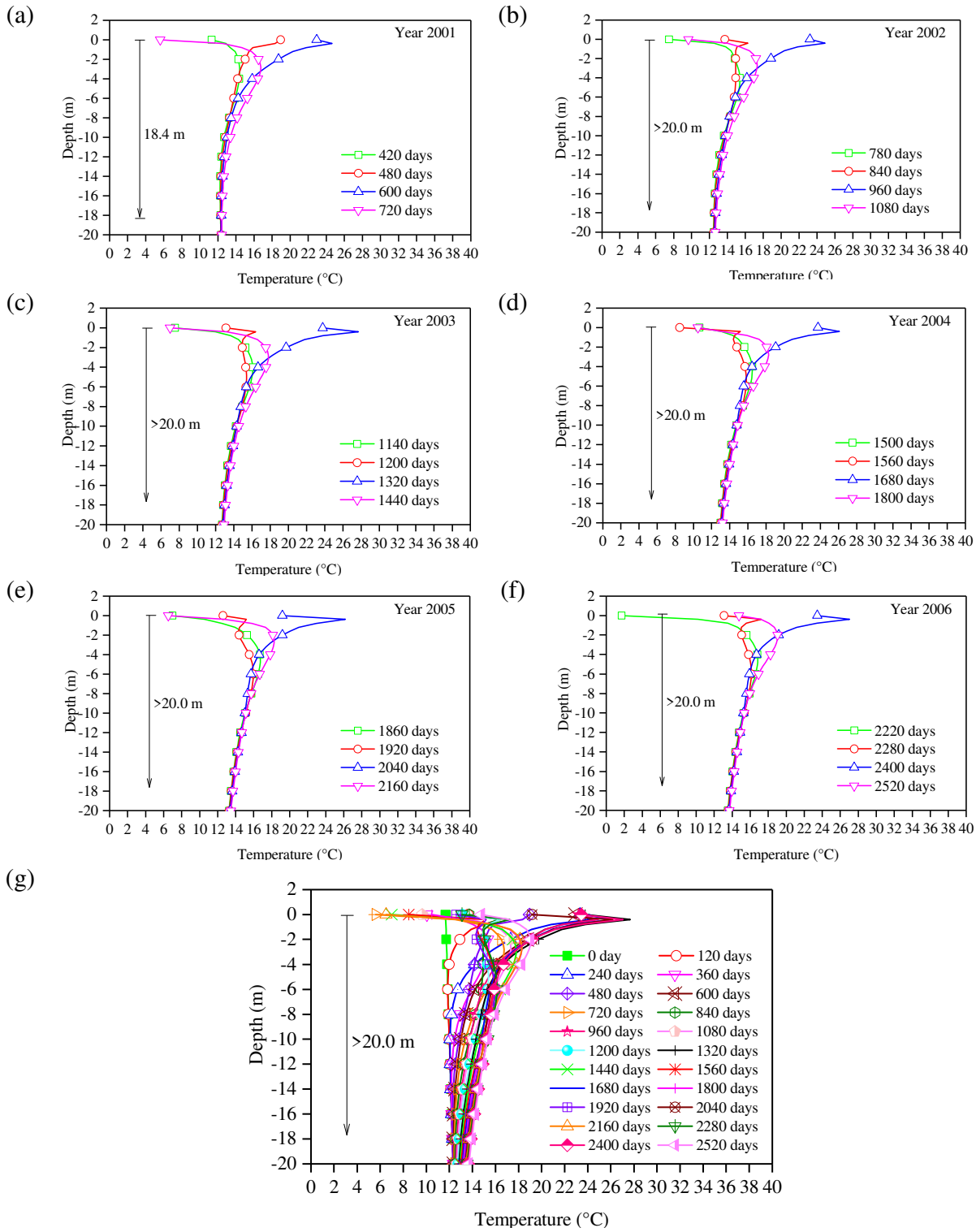

731

732 Figure 13. At the time scale of 30 min, soil temperature profiles at different times in zone 0~-20 m
733 during different studied periods: (a) year 2001, (b) year 2002, (c) year 2003, (d) year 2004, (e) year
734 2005, (f) year 2006, and (g) from year 2000 to 2006